Modeling shock unsteadiness in shock/turbulence interaction

Krishnendu Sinha, Krishnan Mahesh,[a] and Graham V. Candler
Department of Aerospace Engineering and Mechanics, University of Minnesota, 110 Union Street SE, Minneapolis, Minnesota 55455

(Received 25 October 2002; accepted 9 May 2003; published 30 June 2003)

The RANS (Reynolds averaged Navier–Stokes) equations can yield significant error when applied to practical flows involving shock waves. We use the interaction of homogeneous isotropic turbulence with a normal shock to suggest improvements in the $k-\epsilon$ model applied to shock/turbulence interaction. Mahesh *et al.* [J. Fluid Mech. **334**, 353 (1997)] and Lee *et al.* [J. Fluid Mech. **340**, 22 (1997)] present direct numerical simulation (DNS) and linear analysis of the flow of isotropic turbulence through a normal shock, where it is found that mean compression, shock unsteadiness, pressure-velocity correlation, and up-stream entropy fluctuations play an important role in the interaction. Current RANS models based on the eddy viscosity assumption yield very high amplification of the turbulent kinetic energy, k, across the shock. Suppressing the eddy viscosity in a shock improves the model predictions, but is inadequate to match theoretical results at high Mach numbers. We modify the k equation to include a term due to shock unsteadiness, and model it using linear analysis. The dissipation rate equation is similarly altered based on linear analysis results. These modifications improve the model predictions considerably, and the new model is found to match the linear theory and DNS data well. © *2003 American Institute of Physics.* [DOI: 10.1063/1.1588306]

I. INTRODUCTION

The interaction of a turbulent boundary layer with a shock wave is important in many practical flows, e.g., deflected control surfaces of high-speed vehicles and inlet of scram jet engines. Shock/turbulence interactions can cause flow separation and high heating rates, both of which are critical to vehicle design. Commonly studied flow configurations include compression ramps, cylinder-flare combinations, double cones, single or double fins on a plate, oblique shocks impinging on a boundary layer, and transonic airfoils.

Engineering prediction of shock/turbulence interaction relies on Reynolds averaged Navier–Stokes simulations. However, significant disagreement with experimental data is observed even for canonical flows such as the compression ramp. Knight *et al.*[1] summarize results obtained using several turbulence models. Although the predictions are satisfactory for small ramp angles, there is noticeable disagreement with data for higher deflections.[2] The models cannot predict the size of the separation region, the peak heat transfer rate at reattachment, and the mean velocity profiles on the ramp.[2,3] Some attempts have been made to improve the predictions, e.g., realizability constraint,[2] compressibility correction,[3,4] length-scale modification,[4] and rapid compression correction.[4] The outcome of the modifications vary from model to model and also with the test conditions, which point to the possibility that some key physical processes are either modeled incorrectly or not included in the models.

The shock-wave/turbulent boundary layer interaction is complicated by the simultaneous presence of flow separation, stream-line curvature, and mean compression downstream of the shock. By comparison, the interaction of homogeneous isotropic turbulence with a normal shock wave is a simpler and more fundamental problem. Also, direct numerical simulations (DNS) and linear analysis solutions exist for isotropic turbulence interacting with a shock,[5,6] which make it ideal for identifying the important physical mechanisms. It is found that mean compression, shock unsteadiness, pressure-velocity correlation, and entropy fluctuations in the upstream flow play an important role in the interaction.[5,7] Some of these effects are not included in the existing turbulence models, which may be one of the reasons for their inaccuracies. The objective of this paper is to evaluate the $k-\epsilon$ modeling of homogeneous turbulence/shock-wave interaction, and to suggest improvements using linear analysis. The turbulence upstream of the shock is assumed to be essentially composed of vortical fluctuations, i.e., the effect of entropy and acoustic fluctuations is not considered.

The paper is organized as follows. Section II applies the standard $k-\epsilon$ model[8] to the interaction of homogeneous isotropic turbulence with a normal shock wave. The model predictions are compared to DNS and linear analysis, and significantly higher amplification of the turbulent kinetic energy is observed. Recently proposed modifications[9] that suppress eddy viscosity in a shock are found to improve predictions but still do not match the linear theory and DNS. Section III uses linear analysis to improve the $k-\epsilon$ model applied to shock/turbulence interaction. The k equation is modified in Sec. III A to include the effect of shock unsteadiness, and linear analysis is used to model this term. Section III B modifies the dissipation-rate equation in a similar way. The new model is used to predict the interaction of homogeneous tur-

[a]Electronic mail: mahesh@aem.umn.edu

bulence with a normal shock wave in Sec. IV, and is found to reproduce DNS data[5,6] well.

II. CURRENT RANS MODELS

The $k-\epsilon$ model is used to predict the interaction of a Mach 1.29 normal shock with homogeneous isotropic turbulence at Reynolds number based on the Taylor micro-scale, Re_λ, of 19.1 and turbulent Mach number, M_t, of 0.14. Here, $\mathrm{Re}_\lambda = u_{\mathrm{rms}}\lambda/\overline{\nu}$ and $M_t = \sqrt{2k}/\tilde{a}$, where u_{rms} is the rms velocity, λ is the Taylor micro-scale, $\overline{\nu}$ is the mean kinematic viscosity of the fluid, and $\tilde{a}$ is the mean speed of sound. Direct numerical simulation of this flow is presented by Mahesh *et al.*[5]

A. Standard $k-\epsilon$ model

We use the standard $k-\epsilon$ model[8] with the compressible dissipation and pressure-dilatation corrections. In a steady one-dimensional mean flow through a normal shock, the modeled transport equations for the turbulent kinetic energy, k, and the solenoidal dissipation rate, ϵ_s, simplify to

$$\overline{\rho}\tilde{u}\frac{\partial k}{\partial x} = -\widetilde{\overline{\rho}u''u''}\frac{\partial \tilde{u}}{\partial x} - \overline{\rho}(\epsilon_s + \epsilon_c) + \overline{p'\theta'}, \tag{1}$$

$$\overline{\rho}\tilde{u}\frac{\partial \epsilon_s}{\partial x} = -c_{\epsilon 1}\widetilde{\overline{\rho}u''u''}\frac{\partial \tilde{u}}{\partial x}\frac{\epsilon_s}{k} - c_{\epsilon 2}\frac{\epsilon_s^2}{k}, \tag{2}$$

where $k = \frac{1}{2}\widetilde{u_i''u_i''}$, ρ is density, and u is the component of velocity in the streamwise direction, x. Here, the overbar and tilde represent Reynolds and Favre-averaged quantities, and the prime and double-prime represent the Reynolds and Favre fluctuations, respectively. The first and second terms on the right-hand side of the two equations correspond to the production and dissipation mechanisms, and the last term in Eq. (1) is the pressure-dilatation correlation, where p is the pressure and $\theta = u_{i,i}$ is the dilatation. Note that the turbulent transport and viscous diffusion terms are assumed to be small compared to the production and dissipation mechanisms, and are therefore neglected. The normal Reynolds stress, $\widetilde{\overline{\rho}u''u''}$, is modeled using the Boussinesq approximation as

$$\widetilde{\overline{\rho}u''u''} = -\frac{4}{3}\mu_T\frac{\partial \tilde{u}}{\partial x} + \frac{2}{3}\overline{\rho}k, \tag{3}$$

where μ_T is the eddy viscosity and is given by

$$\mu_T = c_\mu\frac{\overline{\rho}k^2}{\epsilon_s}. \tag{4}$$

Here $c_\mu = 0.09$, $c_{\epsilon 1} = 1.35$, and $c_{\epsilon 2} = 1.8$ are model constants, and we use the values given by Chien.[10] The compressible dissipation rate, ϵ_c, and the pressure-dilatation term are modeled as[11,12]

$$\begin{aligned}\epsilon_c &= \alpha_1 M_t^2\epsilon_s,\\ \overline{p'\theta'} &= \alpha_2 M_t^2\widetilde{\overline{\rho}u''u''}\frac{\partial \tilde{u}}{\partial x} + \alpha_3 M_t^2\epsilon_s,\end{aligned} \tag{5}$$

TABLE I. Mean and turbulent flow quantities for the interaction of homogeneous turbulence with a normal shock.

M_1	M_t	Re_λ	k_{in}	ϵ_{in}
1.29	0.14	19.1	9.8×10^{-3}	1.3×10^{-3}
2.0	0.11	19.0	6.6×10^{-3}	6.0×10^{-3}
3.0	0.11	19.7	6.6×10^{-3}	5.7×10^{-3}

where $\alpha_1 = 1$, $\alpha_2 = 0.4$, and $\alpha_3 = 0.2$. Similar to DNS, the model equations are normalized using upstream values of $\overline{\rho}$, $\tilde{a}$, and $\overline{\mu}$, where $\overline{\mu}$ is the mean viscosity of the fluid. In the absence of any physical length scale in the mean flow, an arbitrary length scale is used as reference such that the Reynolds number based on the reference quantities is 750. The normalized inlet values of k and ϵ_s are obtained from the DNS[5] and are listed in Table I. Equations (1) and (2) are integrated through the shock which is specified as hyperbolic tangent profiles of the mean flow quantities with the mean shock thickness taken from DNS.[5]

The evolution of turbulent kinetic energy is shown in Fig. 1, where the data are normalized by the value of k immediately upstream of the shock. The DNS data show very high levels of k at the shock location ($x = 2$). This is an artifact of the unsteady motions of the shock, and does not represent amplification of the turbulent kinetic energy. There is rapid drop and rise in k immediately downstream of the shock (up to $x \simeq 2.7$). This variation is caused by the transfer of energy between the acoustic and vortical modes.[13] Further downstream of the shock, k decreases monotonically due to turbulent dissipation. The $k-\epsilon$ model yields a higher amplification of k across the shock than the DNS. This is because the production term ($\propto 1/\delta^2$, δ being the shock thickness) becomes very large in the shock. Also, the pressure-dilatation term (modeled in terms of production) assumes very large negative values. A balance between these two terms results in high levels of k downstream of the shock. The dissipation term is found to have a negligible contribution in the shock.

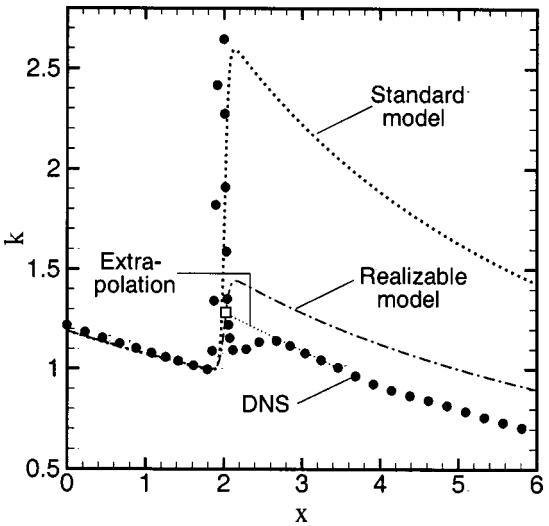

FIG. 1. Evolution of k in the interaction of homogeneous turbulence with a Mach 1.29 normal shock. Different $k-\epsilon$ models are compared to DNS (Ref. 5). (□) The extrapolation of the DNS data for comparison with linear analysis.

The unsteady motion of the shock results in a mean shock thickness that is much larger than that of a steady shock at the same mean flow conditions. The $k-\epsilon$ model does not account for the effect of shock unsteadiness, and therefore cannot predict the shock thickness correctly. In a simulation, the shock thickness depends on the numerics of the computation and the resolution of the grid in the vicinity of the shock. The effect of different numerical methods and grid refinement can be studied in the above-presented test flow by varying the shock thickness in the prescribed mean flow profiles. It is found that the amplification of k and ϵ_s increase very rapidly as the shock becomes thinner due to the nonphysical $1/\delta^2$ variation of the production and pressure-dilatation terms.

B. Realizable $k-\epsilon$ model

In order to reduce the production of k in a shock, several researchers have proposed modifications to the standard model based on the realizability constraint, $0 \leqslant \widetilde{u''u''} \leqslant 2k$, that reduce the eddy viscosity in a shock wave. Here, we present the modification used by Thivet *et al.*[9] where c_μ in the turbulent eddy viscosity expression (4) is given by

$$c_\mu = \min(c_\mu^0, \sqrt{c_\mu^0}/s), \tag{6}$$

where $c_\mu^0 = 0.09$ is the standard value of the constant, and s is a dimensionless mean strain rate, given by $s = Sk/\epsilon_s$ with $S^2 = 2S_{ij}S_{ji} - \frac{2}{3}S_{kk}^2$ and $S_{ij} = \frac{1}{2}(\tilde{u}_{i,j} + \tilde{u}_{j,i})$. Thus, the eddy viscosity in a normal shock becomes

$$\mu_T = \frac{\sqrt{3c_\mu^0}}{2} \frac{\overline{\rho} k}{\partial \tilde{u}/\partial x},$$

which results in

$$\widetilde{u''u''} = 0.35\,k + \tfrac{2}{3}k. \tag{7}$$

Using this expression in place of Eq. (3) yields a much lower amplification of k at the shock ($x=2$) as compared to the standard $k-\epsilon$ model (Fig. 1). The realizable $k-\epsilon$ models proposed by Durbin[14] and Shih *et al.*[15] give similar results. Thus, the modifications based on the realizability constraint give the correct trend by reducing eddy viscosity in the shock, but the model predictions are still higher than the DNS data.

As pointed out earlier, the turbulent dissipation rate has a negligible effect on the evolution of k and ϵ_s across the shock. Also, in case of the realizable $k-\epsilon$ model, pressure-dilatation is small compared to production because $M_t^2 \ll 1$ [see Eq. (5)]. Thus, the amplification of turbulence across the shock is mainly due to the production terms in Eqs. (1) and (2), which can be integrated to get

$$\frac{k_2}{k_1} = \left(\frac{\tilde{u}_1}{\tilde{u}_2}\right)^{2/3+0.35}, \quad \frac{\epsilon_{s2}}{\epsilon_{s1}} = \left(\frac{\tilde{u}_1}{\tilde{u}_2}\right)^{c_{\epsilon 1}(2/3+0.35)}, \tag{8}$$

where subscripts 1 and 2 refer to the state immediately upstream and downstream of the shock wave. Unlike the standard $k-\epsilon$ model, the realizable model yields an amplification of k and ϵ_s that are independent of the numerics or the grid resolution. The amplifications depend only on the upstream mean Mach number.

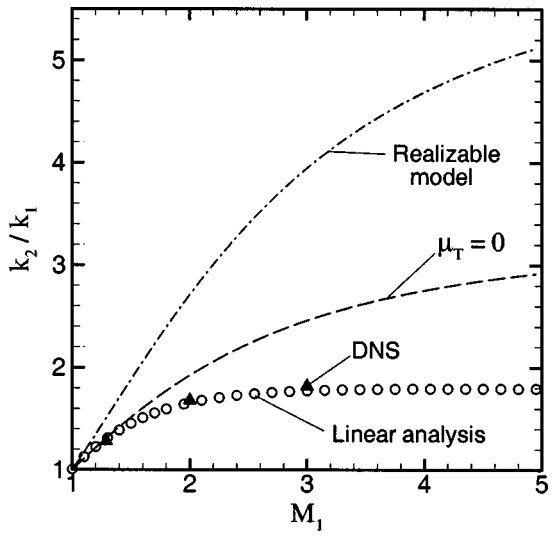

FIG. 2. Amplification of k across a normal shock wave as a function of the upstream mean Mach number. Results obtained from linear analysis (Ref. 5), DNS (Refs. 5 and 6), the realizable $k-\epsilon$ model, and the $k-\epsilon$ model with $\mu_T = 0$.

Mahesh *et al.*[5,7] and Lee *et al.*[6] use linear inviscid analysis to study shock/turbulence interaction. In this approach, the linearized Euler equations are solved for the interaction of homogeneous turbulence with a normal shock. The shock wave is modeled as a discontinuity, and the homogeneous turbulence upstream of the shock is represented as a superposition of Fourier modes, each of which independently interacts with the shock. The analysis predicts an amplification of k across the shock followed by a rapid spatial variation, which is similar to that observed in DNS.[5,6] However, the inviscid theory cannot reproduce the viscous decay in k, and asymptotes to a constant value. Figure 2 shows the ratio of the asymptotic value of k to the upstream turbulent kinetic energy as a function of the upstream normal Mach number, M_1. The theoretical amplification can be compared to DNS data by extrapolating the downstream monotonic decay in k back to the shock location (shown by an open box in Fig. 1). The amplification ratios obtained from the DNS data[5,6] for upstream Mach numbers of 1.29, 2.0, and 3.0 are shown in Fig. 2, and they match the linear analysis results very well.

The amplification of k predicted by the realizable $k-\epsilon$ model for different upstream Mach numbers, Eq. (8), is also shown in Fig. 2. The model yields large amplifications of k, over-predicting the linear analysis results by a factor of 3 or more at large Mach numbers. The amplification of k obtained from the standard $k-\epsilon$ model depends on the shock thickness, and therefore grid independent results cannot be obtained for different Mach numbers.

C. Suppression of eddy viscosity

In a turbulent flow that is in local equilibrium with the mean flow, the Reynolds stresses are linearly related to the mean strain rates via the eddy viscosity. This model works

very well in cases where the turbulent time scale is of the same order in magnitude as the time scale of the mean strain, e.g., a zero pressure gradient boundary layer. However, in a highly nonequilibrium flow, such as a shock/turbulence interaction, the time scale of the mean distortion is significantly smaller than that of the turbulence. Thus, the equilibrium concept of the eddy viscosity breaks down, and the usual model with μ_T given by (4) yields unrealistically high values of the Reynolds stresses, which in turn results in very high production of k. One means of reducing this error is to suppress μ_T entirely within a rapid compression, such that $\widetilde{u''u''}=\frac{2}{3}k$. Using this expression in Eqs. (1) and (2) results in lower amplification of k than the realizable model,

$$\frac{k_2}{k_1}=\left(\frac{\tilde{u}_1}{\tilde{u}_2}\right)^{2/3}, \quad \frac{\epsilon_{s2}}{\epsilon_{s1}}=\left(\frac{\tilde{u}_1}{\tilde{u}_2}\right)^{(2/3)c_{\epsilon 1}}. \tag{9}$$

Here the dissipation and pressure-dilatation terms are neglected because they are small compared to the production in the shock. Note that the amplification ratios depend only on the upstream mean Mach number normal to the shock. Figure 2 shows that the ratio k_2/k_1 given above matches the linear analysis results for $M_1<1.5$ but is significantly higher than the theoretical amplification ratio for higher Mach numbers. This shows that setting $\mu_T=0$, which can be viewed as an extreme limit of the c_μ-correction (6), is not sufficient to get the correct amplification of k.

III. MODELING IMPROVEMENTS

In this section, we present modifications to the existing $k-\epsilon$ model applied to shock/turbulence interactions. The effect of shock unsteadiness on the evolution of k is included in the k equation and is modeled using linear analysis. The modified k equation yields significant improvement over the existing models and the solution matches linear analysis well. The dissipation rate equation is also corrected to predict the amplification of ϵ_s accurately.

A. Turbulent kinetic energy

The evolution of the turbulent kinetic energy in a shock/turbulence interaction is governed by several processes including mean compression, unsteady shock motion, and pressure transport. In order to account for the unsteady motion of the shock, we write a transport equation for k in the frame of reference of the instantaneous shock. The different source terms in the equation are identified and modeled using linear analysis results.

The distortion of the shock from its mean position can be written as $x=\xi(y,z,t)$, where x is the direction normal to the shock. Thus, the linear velocity of the shock in the streamwise direction is ξ_t, and the angular distortions are ξ_y and ξ_z in the $x-y$ and $x-z$ planes. Assuming that the shock undergoes small deviations from its mean position, we can write the linearized conservation equations in a frame of reference that is attached to the shock,

$$\begin{aligned}&\frac{\partial}{\partial x}\rho(u-\xi_t)=0, \quad \rho(u-\xi_t)\frac{\partial u}{\partial x}+\frac{\partial p}{\partial x}=0,\\ &\rho(u-\xi_t)\frac{\partial}{\partial x}(v+\tilde{u}\xi_y)=0,\end{aligned} \tag{10}$$

where $u=\tilde{u}+u''$ is the streamwise velocity, and $v=v''$ and $w=w''$ are the transverse velocity components. Note that w follows an equation very similar to that of v. Here, we assume that the shock-normal derivatives are much larger than the derivatives in a direction parallel to the shock, and that the viscous terms are negligible.

A transport equation for $\widetilde{u''^2}$ can be derived from the streamwise momentum equation. By neglecting the higher-order terms, we get

$$\bar{\rho}\tilde{u}\frac{\partial}{\partial x}\frac{\widetilde{u''^2}}{2}=-\bar{\rho}\widetilde{u''^2}\frac{\partial\tilde{u}}{\partial x}+\bar{\rho}\widetilde{u''\xi_t}\frac{\partial\tilde{u}}{\partial x}-\overline{u''}\frac{\partial\bar{p}}{\partial x}-\overline{u'p'_{,x}}, \tag{11}$$

where the first term on the right-hand side is the production due to mean compression, and the second term represents the effect of shock unsteadiness. They are denoted by P_k and S_k^1, respectively. A positive fluctuation in streamwise velocity $(u''>0)$ upstream of the shock pushes the shock downstream $(\xi_t>0)$ and vice versa. Thus, there is an in-phase coupling between the shock motion and the turbulent fluctuations in the incoming flow. As a result, the net change in the upstream velocity with respect to the shock is smaller than u'', which leads to reduced amplification in u'' through the shock. Linear analysis shows that $\widetilde{u''\xi_t}>0$, and therefore S_k^1 reduces the amplification of $\widetilde{u''^2}$ through the shock. The third term on the right-hand side is the production due to mean pressure gradient, and it represents the effect of entropy fluctuations on the flow. The last term, denoted by Π_k^1, represents the effect of the pressure-velocity correlation on the evolution of $\widetilde{u''^2}$.

A transport equation for $\widetilde{v''^2}$ can be derived from the transverse momentum equation,

$$\bar{\rho}\tilde{u}\frac{\partial}{\partial x}\frac{\widetilde{v''^2}}{2}=-\bar{\rho}\tilde{u}\widetilde{v''\xi_y}\frac{\partial\tilde{u}}{\partial x}, \tag{12}$$

where the term on the right-hand side, denoted by S_k^2, represents the effect of shock distortion. Across a distorted shock, a sum of v'' and the component of mean flow tangential to the shock, $\tilde{u}\xi_y$, is conserved. A decrease in $\tilde{u}$ across the shock results in a change in $\widetilde{v''^2}$. Linear analysis shows that $\widetilde{v''\xi_y}>0$ such that shock distortion amplifies $\widetilde{v''^2}$ across the shock. Note that $\widetilde{w''^2}$ follows an equation similar to (12).

Using the linearized Rankine–Hugoniot relations presented by Mahesh *et al.*,[5] we can write an equation for the change in $\overline{u'^2}$ across the shock,

$$\begin{aligned}\bar{\rho}_1\bar{u}_1\tfrac{1}{2}(\overline{u_2'^2}-\overline{u_1'^2})=&-\bar{\rho}_1\overline{u_1'u_m'}\Delta\bar{u}+\bar{\rho}_1\overline{u_m'\xi_t}\Delta\bar{u}+\overline{\rho_1'u_m'}(\bar{p}_2\\ &-\bar{p}_1)/\bar{\rho}_1-\overline{u_m'(p_2'-p_1')},\end{aligned} \tag{13}$$

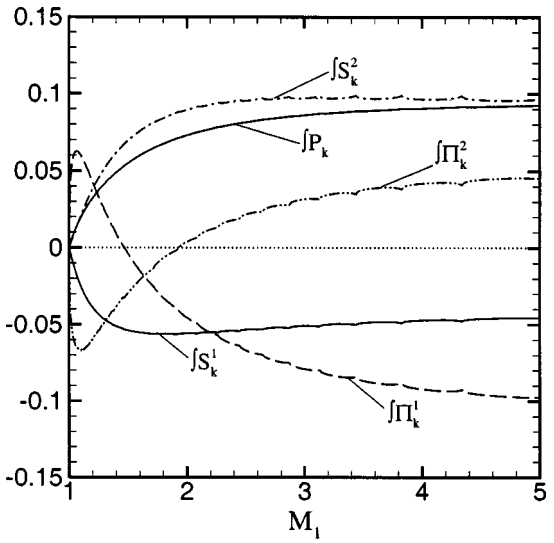

FIG. 3. Budget of Eqs. (13) and (14) at different Mach numbers: P_k=production, S_k^1=shock unsteadiness term, S_k^2=shock distortion term, Π_k^1=pressure-velocity term, and $\int$ represents the integration across the shock. $\int\Pi_k^2$ is the total contribution of the energy exchange mechanism downstream of the shock. All terms are normalized by $\overline{\rho}_1\overline{u}_1^3$.

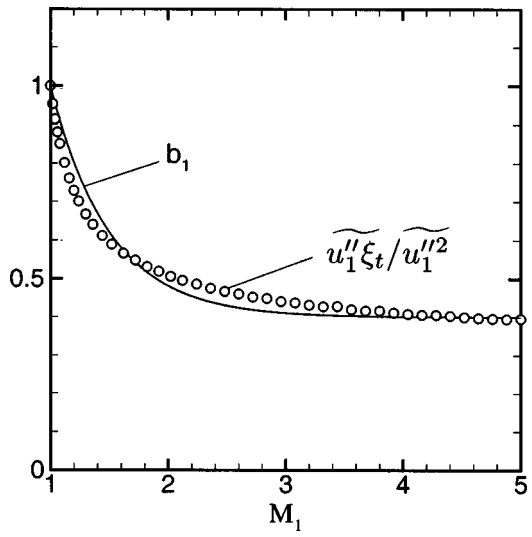

FIG. 4. The ratio $\widetilde{u_1''\xi_t}/\widetilde{u_1''^2}$ predicted by linear analysis (Ref. 5) is used to obtain the modeling coefficient, b_1.

where $\Delta\overline{u}=\overline{u}_2-\overline{u}_1$ and $u_m'=\frac{1}{2}(u_1'+u_2')$. The above equation can be interpreted as an integrated form of Eq. (11), where the first two terms on the right-hand side correspond to the production and shock unsteadiness mechanisms. The third term is the production due to mean pressure gradient and the last term represents the effect of pressure-velocity correlation on the flow. Note that $u''=u'$ and $\tilde{u}=\overline{u}$ in the linear limit. Similarly, we can write an equation for the change in $\overline{v'^2}$,

$$\overline{\rho}_1\overline{u}_1\tfrac{1}{2}(\overline{v_2'^2}-\overline{v_1'^2})=-\overline{\rho}_1\overline{u}_1\overline{\tfrac{1}{2}(v_1'+v_2')\xi_y}\Delta\overline{u}, \tag{14}$$

which can be viewed as an integrated form of Eq. (12).

Figure 3 shows a budget of Eq. (13) for different Mach numbers where the terms are normalized by $\overline{\rho}_1\overline{u}_1^3$. We consider purely vortical turbulence upstream of the shock, and hence $\rho_1'=p_1'=T_1'=0$. As a result, the production due to mean pressure gradient is identically zero. The production due to mean compression is positive, while shock unsteadiness reduces $\overline{u'^2}$. The pressure-velocity term has a significant contribution to the overall budget. The shock distortion term is also shown in the figure, and it has an amplifying effect on the turbulent kinetic energy.

Mahesh *et al.*[13] show that the total energy in the linearized disturbances remains constant downstream of the shock, i.e.,

$$\frac{\gamma M}{2}\left[\frac{2k}{\tilde{a}^2}+\frac{\overline{p'^2}}{\gamma^2\overline{p}^2}\right]+\frac{\overline{p'u'}}{\overline{p}\tilde{a}}=\text{const.} \tag{15}$$

The interaction of vortical turbulence with a shock produces acoustic energy, i.e., $\overline{p'^2}\neq 0$ and $\overline{p'u'}\neq 0$ immediately behind the shock. The majority of the acoustic energy decays rapidly downstream of the shock, and it is transferred to the vortical mode so that the total energy is conserved. The change in k due to this energy transfer mechanism is denoted by a source term, Π_k^2, in the k equation. The total contribution of this energy exchange mechanism is plotted as a function of the upstream Mach number in Fig. 3.

The different mechanisms discussed above can be combined with the turbulent dissipation rate, ϵ, to get an equation for the turbulent kinetic energy,

$$\overline{\rho}\tilde{u}\frac{\partial k}{\partial x}=P_k+S_k^1+2S_k^2+\Pi_k^1+\Pi_k^2-\overline{\rho}\epsilon, \tag{16}$$

that governs the interaction of homogeneous isotropic turbulence with a normal shock. Here, the production due to mean pressure gradient is neglected, and a factor of 2 multiplies S_k^2 in order to include the shock distortion effects on $\widetilde{w''^2}$.

The modeling of Eq. (16) is described in the following. The shock-unsteadiness term is a function of $\widetilde{u''\xi_t}$, which is modeled as

$$\widetilde{u''\xi_t}=b_1\widetilde{u''^2}, \tag{17}$$

where b_1 is a modeling coefficient. This is based on the assumption that the unsteadiness of the shock is caused by the turbulent fluctuations in the flow. We use

$$b_1=0.4+0.6e^{2(1-M_1)}, \tag{18}$$

which is a curve-fit to the ratio $\widetilde{u_1''\xi_t}/\widetilde{u_1''^2}$ obtained from linear analysis (Fig. 4). Thus,

$$S_k^1=\overline{\rho}\widetilde{u''^2}\frac{\partial\tilde{u}}{\partial x}b_1. \tag{19}$$

The terms S_k^2, Π_k^1, and Π_k^2 are functions of $\widetilde{v''\xi_y}$, $\overline{p'^2}$, and $\overline{p'u'}$. These correlations can be modeled by introducing additional coefficients, similar to b_1. However, we take a simpler approach where the model for S_k^1 is included in Eq. (16), while S_k^2, Π_k^1, and Π_k^2 are neglected. The effect of this simplification is discussed in the following. Thus, we get

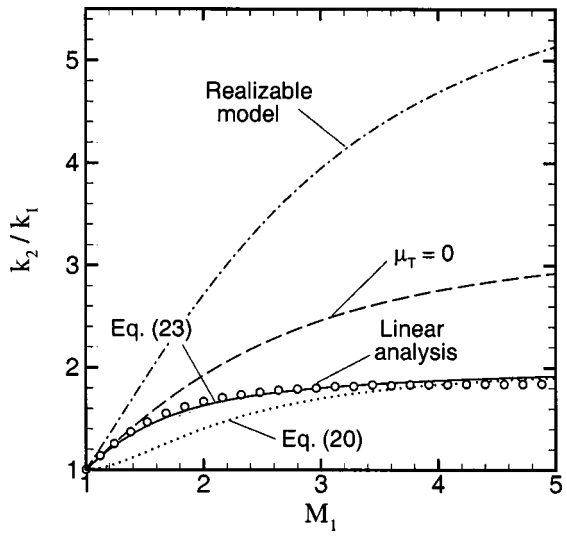

FIG. 5. Turbulent kinetic energy amplification in a shock/turbulence interaction as a function of the upstream Mach number. Different $k-\epsilon$ models are compared to linear analysis (Ref. 5).

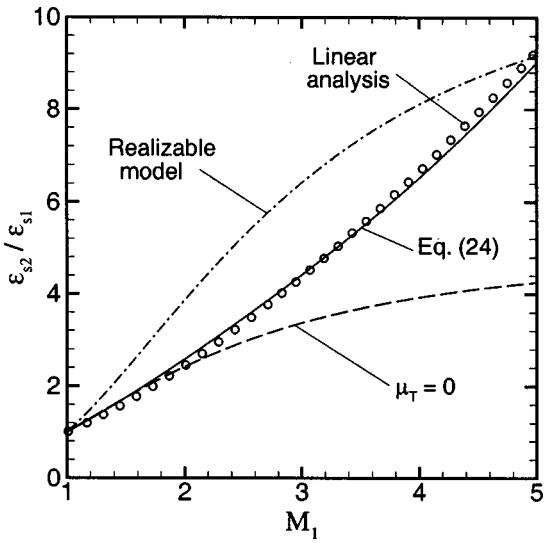

FIG. 6. Amplification in solenoidal dissipation rate in a shock/turbulence interaction as a function of the upstream Mach number. Different $k-\epsilon$ models are compared with linear analysis (Ref. 5).

$$\overline{\rho}\widetilde{u}\frac{\partial k}{\partial x} = -\overline{\rho}\widetilde{u''^2}\frac{\partial \widetilde{u}}{\partial x}(1-b_1) - \overline{\rho}\epsilon. \tag{20}$$

Using the isotropic form of the normal Reynolds stress $\widetilde{u''^2} = \frac{2}{3}k$, as obtained by setting $\mu_T = 0$ in Eq. (3), and integrating the above-modeled equation across the shock results in

$$\frac{k_2}{k_1} = \left(\frac{\widetilde{u}_1}{\widetilde{u}_2}\right)^{(2/3)(1-b_1)}. \tag{21}$$

Here the effect of the viscous dissipation is neglected in the shock. Figure 5 compares the above result to linear analysis. For $M_1 > 3$, the model approximately matches linear theory, which implies that Eq. (20) with $\mu_T = 0$ reproduces the overall effect of all the terms in Eq. (16), including S_k^2, Π_k^1, and Π_k^2, for high Mach number flows.

For $M_1 < 3$, the above model yields a lower k_2/k_1 than the linear analysis. This is because b_1 approaches 1 at low Mach numbers such that S_k^1 cancels the amplification of k due to P_k. The budget of the source terms in Fig. 3 shows that for $M_1 < 2$, $S_k^1 \cong -P_k$ and that the contributions of the other terms result in a net amplification of k. Thus, the effect of S_k^2, Π_k^1, and Π_k^2 needs to be included at low Mach numbers. This can be achieved by reducing the value of b_1 in Eq. (20). Also, $b_1 \to 1$ as $M_1 \to 1$ causes the model to yield the wrong asymptotic behavior in this limit (see Fig. 5). Specifically, for $M_1 \cong 1$, linear analysis yields $k_2/k_1 = 1 + \mathcal{O}(M_1 - 1)$ whereas Eq. (20) predicts $k_2/k_1 = 1 + \mathcal{O}(M_1 - 1)^2$. It is reasonable to assume that the combined effect of the source terms due to shock/turbulence interaction, namely S_k^1, S_k^2, Π_k^1, and Π_k^2, vanish at $M_1 = 1$. This can be achieved by replacing b_1 in Eq. (20) by b_1', where b_1' is obtained by modifying b_1 with an exponential function between the limits of $M_1 = 1$ and $M_1 \to \infty$,

$$b_1' = b_{1,\infty}(1 - e^{1-M_1}). \tag{22}$$

Here $b_{1,\infty} = 0.4$ is the high Mach number limiting value of b_1. Thus, $b_1' \to b_1$ in the high Mach number limit, and for low Mach numbers, we have $b_1' < b_1$ so as to include the effect of S_k^2, Π_k^1, and Π_k^2. The final model equation for k can therefore be written in a frame-independent form as

$$\overline{\rho}\widetilde{u}_i\frac{\partial k}{\partial x_i} = -\frac{2}{3}\overline{\rho}kS_{jj}(1-b_1') - \overline{\rho}\epsilon. \tag{23}$$

Integration of Eq. (23) across a shock (with $\epsilon = 0$) yields k_2/k_1 which has a form similar to Eq. (21). Figure 5 shows that the amplification of k predicted by the above equation matches the linear theory results over the entire range of Mach numbers.

B. Turbulent dissipation rate

The turbulent dissipation rate consists of a solenoidal part, a compressible part, and contributions due to inhomogeneity and fluctuations in viscosity. We assume that the solenoidal dissipation rate given by $\epsilon_s = \overline{\nu}\overline{\omega_i'\omega_i'}$ is the dominant part, where ω' is the vorticity fluctuation. Mahesh *et al.*[5] and Lee *et al.*[6] show that the vorticity components transverse to the shock are amplified, and the streamwise component remains unchanged. Also, $\overline{\nu}$ changes across the shock due to an increase in mean temperature and mean density. We combine the amplification of $\overline{\omega_i'\omega_i'}$ predicted by linear analysis with the change in $\overline{\nu}$ to obtain the amplification of ϵ_s across the shock (Fig. 6). The results of the realizable $k-\epsilon$ model [Eq. (8)] and the $k-\epsilon$ model with $\mu_T = 0$ [Eq. (9)] are also presented in the figure. The realizable model shows a poor comparison with the linear analysis, while the $k-\epsilon$ model with $\mu_T = 0$ is close to the theory up to $M_1 = 2.0$ and under-predicts the amplification of ϵ_s for higher Mach numbers. This may be because of the effect of shock unsteadiness and compressibility, which are not accounted for in the models. In this work, we do not attempt to identify and model all the physical mechanisms that affect the solenoidal dissipation rate. Instead, we modify the model

parameter $c_{\epsilon 1}$ in the ϵ_s equation (with $\mu_T=0$) such that it predicts the correct change in ϵ_s across the shock. We use

$$c_{\epsilon 1}=1.25+0.2(M_1-1), \tag{24}$$

which is tailored to match the linear analysis results for $1<M_1<7$ (Fig. 6).

Note that the modifications proposed in this section are applicable only in a shock wave, and therefore in a subsonic flow $b_1'=0$. This can be achieved by multiplying the expressions for b_1' by the factor $\frac{1}{2}(1+\text{sign}(M_1-1))$. $c_{\epsilon 1}$ can be altered in a similar way so that it retains its original value in a subsonic flow. Also, the modifications are strictly applicable when the flow on either side of the shock is uniform. Application to flows with additional mean gradients may require further modifications and are beyond the scope of this paper.

IV. MODEL EVALUATION

We use the different variations of the $k-\epsilon$ model discussed above to predict the interaction of vortical homogeneous isotropic turbulence with a normal shock at upstream Mach numbers of 1.29, 2.0, and 3.0. DNS data[5,6] showing the evolution of k in these flows are compared to the predictions of the standard model, the realizable model, the model with $\mu_T=0$, and the new model given by Eqs. (23) and (24). The values of Re_λ and M_t for the three test cases are listed in Table I. For the $M_1=1.29$ case, these values correspond to the inlet station, and are used to obtain the inlet values of k and ϵ_s. For $M_1=2$ and 3, the values of M_t and Re_λ are immediately upstream of the shock, which are extrapolated to obtain k and ϵ_s at the inlet using the decay rate of homogeneous turbulence predicted by the standard $k-\epsilon$ model. The normalized inlet values, k_{in} and ϵ_{in}, are listed in Table I. As discussed in Sec. II, the model equations are solved in a normalized form, and the mean flow quantities are specified as hyperbolic tangent profiles with the mean shock thickness taken from DNS. The solution of the standard $k-\epsilon$ model is a strong function of the shock thickness, whereas the amplifications predicted by the other $k-\epsilon$ models do not depend on the shock thickness.

Figure 7 shows the evolution of k in the shock/turbulence interactions, where the data are normalized by the value of k immediately upstream of the shock. The new model matches the DNS amplification of k well in the Mach 1.29 and 3.0 flows, and under-predicts the data in the Mach 2.0 case. On the other hand, the standard and realizable $k-\epsilon$ models yield a much higher level of k downstream of the shock. The model with $\mu_T=0$ predicts the correct amplification of k in the Mach 1.29 flow, but over-predicts the DNS data in the Mach 2 and 3 cases. Note that none of the $k-\epsilon$ models reproduce the rapid variation in k immediately behind the shock because they do not model the decay of the acoustic energy in this region.

The monotonic decay rate of k downstream of the shock is determined by ϵ. The new model matches the theoretical amplification of ϵ_s (see Fig. 6), and yields the correct decay rate in the $M_1=2$ and 3 cases. However, it predicts a slower decay than DNS in the Mach 1.29 flow. The decay rate of k predicted by the model with $\mu_T=0$ is very similar to the new model for the first two test cases and is relatively low in the Mach 3 flow. The realizable model yields a higher amplifi-

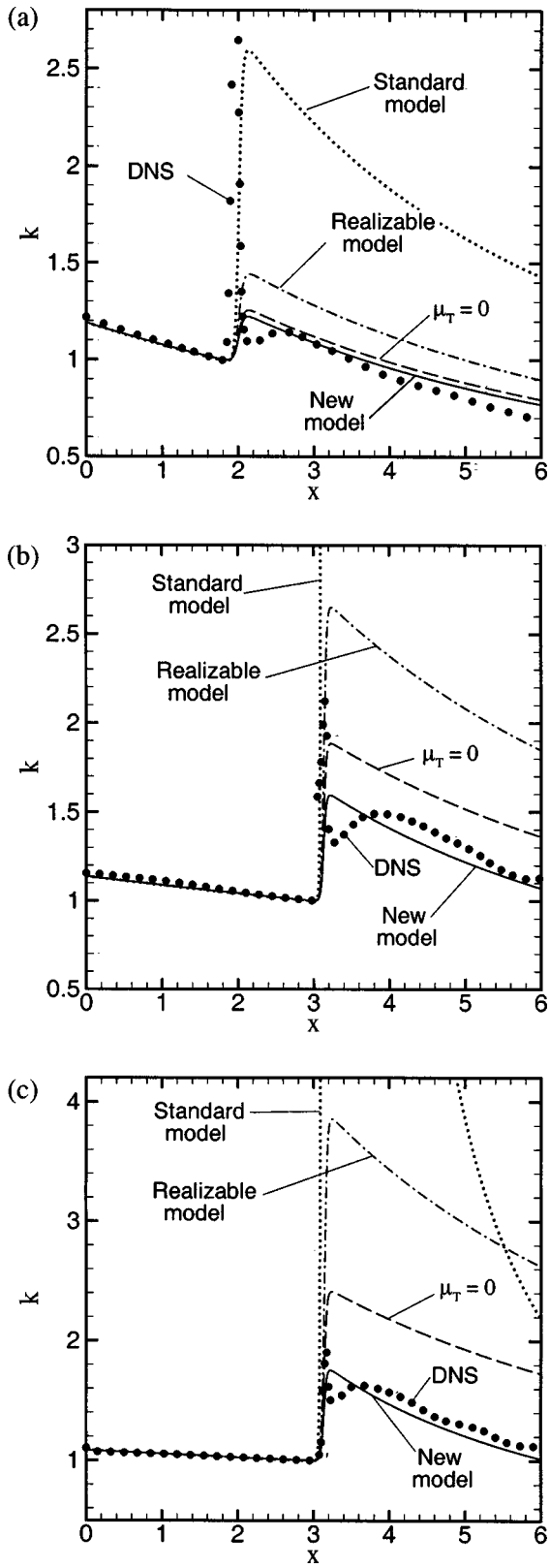

FIG. 7. Evolution of k in the interaction of homogeneous isotropic turbulence with a normal shock at M_1: (a) 1.29, (b) 2.0, and (c) 3.0. Different variations of the $k-\epsilon$ model (lines) are compared with DNS data—Refs. 5 and 6 (symbols).

cation of ϵ_s than the linear analysis for $M_1<5$. The corresponding decay rate appears to match DNS in the Mach 1.29 flow, but is higher than the data in the latter two test cases. The standard $k-\epsilon$ model yields much higher ϵ_s, and therefore results in a significantly higher decay rate of k downstream of the shock.

V. CONCLUSIONS

We study the modeling of homogeneous isotropic turbulence interacting with a normal shock. The standard $k-\epsilon$ model grossly over-predicts the amplification in the turbulent kinetic energy, k, across the shock, because the underlying eddy viscosity assumption breaks down in a rapidly distorting mean flow. Modifications based on the realizability constraint reduce the eddy viscosity, and thus yield a lower amplification in k. However, it is shown that eddy viscosity corrections are not enough to match the linear theory and direct numerical simulation (DNS). This is because the existing models do not account for some of the key physical processes involved in these interactions, e.g., the unsteady motion of the shock wave that is found to reduce the amplification of the turbulent kinetic energy. We modify the k equation to incorporate the shock-unsteadiness mechanism and model it using linear analysis. The resulting equation yields a significant improvement over the existing models. The equation for the solenoidal dissipation rate is also modified so that it predicts the correct amplification of ϵ_s across the shock. The new $k-\epsilon$ model reproduces DNS data of shock/isotropic turbulence interaction well.

ACKNOWLEDGMENTS

We would like to acknowledge support from the Air Force Office of Scientific Research under Grant No. F49620-01-1-0060. This work was also sponsored by the Army High Performance Computing Research Center under the auspices of the Department of the Army, Army Research Laboratory Cooperative Agreement No. DAAD191-01-2-0014, the content of which does not necessarily reflect the position or the policy of the government, and no official endorsement should be inferred. A portion of the computer time was provided by the University of Minnesota Supercomputing Institute.

[1] D. Knight, H. Yan, A. Panaras, and A. Zheltovodov, "RTO WG 10: CFD validation for shock wave turbulent boundary layer interactions," AIAA Pap. 2002-0437 (2002).
[2] W. W. Liou, G. Huang, and T.-H. Shih, "Turbulence model assessment for shock-wave/turbulent boundary layer interaction in transonic and supersonic flows," Comput. Fluids **29**, 275 (2000).
[3] J. Forsythe, K. Hoffmann, and H.-M. Damevin, "An assessment of several turbulence models for supersonic compression ramp flow," AIAA Pap. 98-2648 (1998).
[4] T. J. Coakley and P. G. Huang, "Turbulence modeling for high speed flows," AIAA Pap. 92-0436 (1992).
[5] K. Mahesh, S. K. Lele, and P. Moin, "The influence of entropy fluctuations on the interaction of turbulence with a shock wave," J. Fluid Mech. **334**, 353 (1997).
[6] S. Lee, S. K. Lele, and P. Moin, "Interaction of isotropic turbulence with shock waves: Effect of shock strength," J. Fluid Mech. **340**, 225 (1997).
[7] K. Mahesh, S. Lee, S. K. Lele, and P. Moin, "The interaction of an isotropic field of acoustic waves with a shock wave," J. Fluid Mech. **300**, 383 (1995).
[8] D. C. Wilcox, *Turbulence Modeling for CFD*, 2nd ed. (DCW Industries, La Canada, CA, 1998), p. 236.
[9] F. Thivet, D. D. Knight, A. A. Zheltovodov, and A. I. Maksimov, "Importance of limiting the turbulent stresses to predict 3D shock-wave/boundary-layer interactions," 23rd International Symposium on Shock Waves, Fort Worth, TX, Paper No. 2761, 2001.
[10] K. Y. Chien, "Prediction of channel and boundary-layer flows with a low-Reynolds-number turbulence model," AIAA J. **20**, 33 (1982).
[11] S. Sarkar, G. Erlebacher, M. Y. Hussaini, and H. O. Kreiss, "Analysis and modelling of dilatational terms in compressible turbulence," J. Fluid Mech. **227**, 473 (1991).
[12] S. Sarkar, "The pressure-dilatation correlation in compressible flows," Phys. Fluids A **4**, 2674 (1992).
[13] K. Mahesh, P. Moin, and S. K. Lele, "The interaction of a shock wave with a turbulent shear flow," Thermosciences Division, Department of Mechanical Engineering, Stanford University, Report No. TF-69, Stanford, CA, 1996.
[14] P. A. Durbin, "On the k-3 stagnation point anomaly," Int. J. Heat Fluid Flow **17**, 89 (1996).
[15] T. H. Shih, W. W. Liou, A. Shabbir, Z. Yang, and J. Zhu, "A new $k-\epsilon$ eddy viscosity model for high Reynolds number turbulent flows," Comput. Fluids **24**, 227 (1995).